

# Dynamics at barriers in bidirectional two-lane exclusion processes

**Róbert Juhász**

Research Institute for Solid State Physics and Optics, H-1525 Budapest, P.O.Box 49, Hungary

E-mail: juhasz@szfki.hu

**Abstract.** A two-lane exclusion process is studied where particles move in the two lanes in opposite directions and are able to change lanes. The focus is on the steady state behavior in situations where a positive current is constrained to an extended subsystem (either by appropriate boundary conditions or by the embedding environment) where, in the absence of the constraint, the current would be negative. We have found two qualitatively different types of steady states and formulated the conditions of them in terms of the transition rates. In the first type of steady state, a localized cluster of particles forms with an anti-shock located in the subsystem and the current vanishes exponentially with the extension of the subsystem. This behavior is analogous to that of the one-lane partially asymmetric simple exclusion process, and can be realized e.g. when the local drive is induced by making the jump rates in two lanes unequal. In the second type of steady state, which is realized e.g. if the local drive is induced purely by the bias in the lane change rates, and which has thus no counterpart in the one-lane model, a delocalized cluster of particles forms which performs a diffusive motion as a whole and, as a consequence, the current vanishes inversely proportionally to the extension of the subsystem. The model is also studied in the presence of quenched disorder, where, in case of delocalization, phenomenological considerations predict anomalously slow, logarithmic decay of the current with the system size in contrast with the usual power-law.

PACS numbers: 05.70.Ln, 87.16.aj, 87.16.Uv

## 1. Introduction

Transport in cells is an intensively studied field of cell biology as it is important for cellular organization and function, moreover, malfunction of transport processes may lead to severe diseases [1, 2, 3]. Intracellular transport is realized by a class of proteins called molecular motors which are able to convert chemical energy released from hydrolysis of ATP into mechanical work and thereby perform directed movement on the filament network and carry different cargoes from one part of the cell to the other [2]. Although basic features of this system are well known there are still important details which have not cleared up yet and, for instance, concurring models of bidirectional transport exist currently [3].

This important issue has motivated much theoretical work on special driven lattice gas models which have been used as minimal models of cooperative behavior of molecular motors [4]. The cornerstone of these investigations is the asymmetric simple exclusion process (ASEP) [5, 6] in which particles sitting on a one-dimensional lattice jump stochastically to a neighboring site provided the latter is empty. Due to its simple formulation, this process has become a paradigmatic model of interacting many-particle systems which have nonequilibrium steady-states [7, 8, 9]. The system, when coupled to particle reservoirs at the ends, shows boundary induced phase transitions [10] and the phase diagram is exactly known [11, 12, 13].

The ASEP has been generalized in many different directions in order to take into account more details of real transport systems. Such generalized models are the two or multilane models which consist of two or more ASEPs coupled in parallel, where particles are able to jump to other lanes. Formally, on the grounds of the directionality of the motion in the lanes, these models can be divided in three classes. First, particles move totally asymmetrically (unidirectionally) within lanes and the direction of motion is the same in all lanes [14, 15, 16, 17, 18, 19]. This generalization is inspired by the circumstance that the microtubule filament that serves as a track for certain molecular motors is not strictly one-dimensional but consists of many proto-filaments. Such models have also been investigated in the context of vehicular traffic on multi-lane roads; for a review, see e.g. Ref. [20]. Second, two-lane models with unidirectional motion in one lane and symmetric (diffusive) motion in the other one have also been introduced [21, 22]. These models have been intended to take into consideration that real molecular motors can unbind from the filament, diffuse in the surrounding fluid and rebind again to the filament. The unbinding and rebinding has also been taken into account by simpler models where the ASEP is extended by creation and annihilation of particles [23], as well as by more realistic models where the ASEP is coupled to a finite compartment in which the motion is diffusive [24, 25, 26, 27]. Third, a two-lane model with unidirectional motion in the lanes but with opposite orientation of the lanes has also been studied [28, 29]. This arrangement can be thought of as a simplified model of motors moving along two oppositely oriented filament tracks which are located in a tube-like narrow compartment. The motion of a single particle in this environment has been found to

have an enhanced diffusion coefficient compared to that of the symmetric random walk [29]. This type of active diffusion can be realized experimentally and it is also present *in vivo* [3]. An alternative interpretation of this model is that a single filament is placed in a narrow compartment where there is a steady convection of the medium in the opposite direction compared to the polarity of the filament.

The theoretical studies have concluded that, in all three cases, the steady-state behavior is richer than that of the one-lane ASEP, furthermore, interesting phenomena take place in such systems, for instance, synchronization or localization of density shocks. The latter can be observed experimentally in the traffic of kinesin motors in accordance with theoretical predictions [30, 31, 32].

This work wishes to contribute to the studies on the less examined bidirectional models of the third class. Earlier studies have concentrated either on the one particle dynamics [29] or on the case of weak coupling between the channels, which can be treated by means of a hydrodynamic description [28]. In the present work, the case will be considered where the inter-lane jump rates are comparable with the intra-lane jump rates. A special property of this model is that, under certain conditions, the stationary current can be reversed when the global density of particles is varied. In other words, if particles are present in the system with a sufficiently high density they are able to flow in the opposite direction as a single particle. We shall give the condition of this phenomenon in terms of the transition rates of the process. Subsequently, we shall analyze the quantitative consequences of this property in arrangements where the system contains a finite region where the local bias is opposite to the global one. It will turn out that the steady state at such an inclusion with reverse bias, or “barrier” is qualitatively different from that of the analogous one-lane partially asymmetric simple exclusion process in the reverse bias regime. In the latter model, a shock forms in the middle of the barrier and the stationary current tends to zero exponentially with the size of the barrier [34, 33, 13]. As opposed to this, in the two-lane model to be studied, a shock still appears but, under certain conditions, it may be delocalized, which leads to that the current vanishes much slower: it is inversely proportional to the size of the barrier. A direct consequence of this slow mode is that, in case of quenched disordered lane-change rates, the current  $J$  vanishes with the size of the system  $L$  as  $J(L) \sim (\ln L)^{-1}$  in the presence of a global bias, which is slower than the usual power-law decay characteristic of disordered partially asymmetric one-lane models [35, 36, 37, 38, 39].

The paper is organized as follows. The model will be defined in Sec. 2. The process in the presence of a single particle is studied in Sec. 3. The periodic system and the phases determined by the bulk rates are discussed in Sec. 4. In Sec. 5, the phase diagram of the open system is determined. Sec. 6 is devoted to heterogeneous models including one-barrier systems and random disorder. Some calculations are presented in the Appendix and the results are summarized in Sec. 7.

## 2. The model

The model is defined on two parallel one dimensional lattices with  $L$  sites, denoted by  $A$  and  $B$ , the sites of which are either empty or occupied by a particle. We shall study periodic chains (or rings), where site 1 and  $L$  are neighbors, as well as open chains. The configuration of the system is specified by the set of occupation numbers  $n_l^{A,B}$ ,  $l = 1, 2, \dots, L$ , which are zero (one) for empty (occupied) sites. On the space of configurations, a continuous-time Markov process is defined by the rates of allowed transitions, are the followings for periodic chains. On site  $l$  of lane  $A(B)$ , a particle attempts to jump to the adjacent site on its right(left) hand side with rate  $p_l(q_l)$  and the attempt is successful if the target site is empty. Furthermore, a particle residing at site  $l$  of chain  $A(B)$  jumps to site  $l$  of chain  $B(A)$  with rate  $u_l$  ( $v_l$ ), provided the target site is empty. The model is illustrated in Fig. 1.

For open systems, the above process is modified at surface sites 1 and  $L$  as follows. On the first site of lane  $A$  particles are injected with rate  $\alpha$ , provided this site is empty. On site  $L$  of lane  $A$  particles are deleted with rate  $\gamma$ , whereas on the first site of lane  $B$  they are deleted with rate  $\beta$ . In case of open systems, we restrict ourselves to a homogeneous bulk, i.e.  $p_l = p$ ,  $q_l = q$ ,  $u_l = u$ ,  $v_l = v$ , see Fig. 2. Moreover, we shall focus on the reverse bias regime, where a single particle is driven to the left in the bulk and are mainly interested in under which conditions a positive current can be forced to the system by injecting particles at site 1. For sake of simplicity, particles are not injected at site  $L$  and the exit rate  $\gamma$  at that site is set to 1.

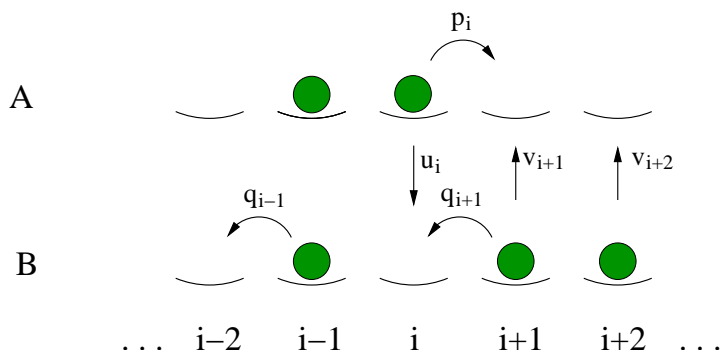


**Figure 1.** Schematic view of the model in the bulk. Arrows indicate the allowed transitions.

## 3. One-particle dynamics

Let us examine the motion of a single particle in the system, a situation which will be relevant for the analysis of the stability of shocks. Although, detailed-balance does not hold in this system as the motion of the particle is unidirectional within the lanes, we shall show that an effective potential can still be defined. Let us consider the steady state of a particle on a finite ring. The probability that the particle is found at site  $i$  of

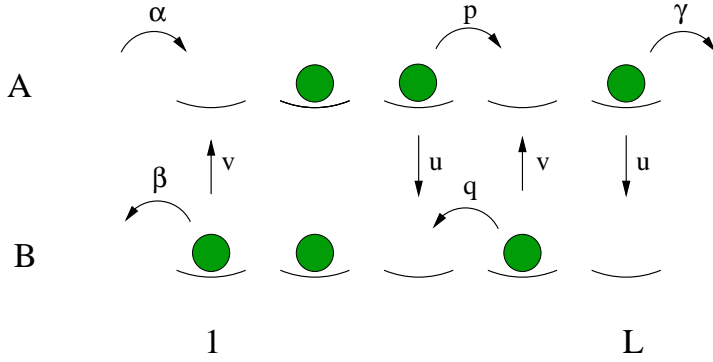


**Figure 2.** Schematic view of the open system. Arrows indicate the allowed transitions.

lane  $A(B)$  is denoted by  $\rho_i(\pi_i)$ . The probability current  $J$  flowing parallel to the lanes (see Fig. 3) can be written as

$$J = p_{i-1}\rho_{i-1} - q_i\pi_i. \quad (1)$$

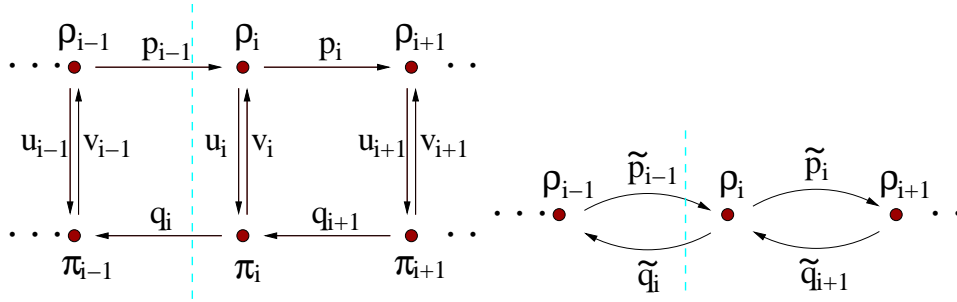


**Figure 3.** Left: stationary probabilities on a finite ring with a single particle. Right: partially asymmetric one-lane model obtained by the elimination of lane  $B$ . The stationary current across the dashed line is denoted by  $J$ .

Conservation of probability at site  $i$  of lane  $A$  and  $B$  imply

$$p_{i-1}\rho_{i-1} + v_i\pi_i - (p_i + u_i)\rho_i = 0 \quad (2)$$

$$q_{i+1}\pi_{i+1} + u_i\rho_i - (q_i + v_i)\pi_i = 0. \quad (3)$$

Let us assume that  $v_i > 0$  for  $i = 1, 2, \dots, L$ . Expressing  $\pi_i$  from Eq. (2) and substituting into Eq. (1) we obtain

$$J = \tilde{p}_{i-1}\rho_{i-1} - \tilde{q}_i\rho_i, \quad (4)$$

where  $\tilde{p}_{i-1} = p_{i-1}(q_i + v_i)/v_i$  and  $\tilde{q}_i = q_i(p_i + u_i)/v_i$ . Formally, this equation is identical to that describing the stationary current in a one-lane partially asymmetric model with forward and backward rates  $\tilde{p}_i$  and  $\tilde{q}_i$ , see Fig. 3. This correspondence with a one-lane model is not perfect as the occupations  $\rho_i$  alone are not normalized to one, i.e.  $\sum_{i=1}^L \rho_i < \sum_{i=1}^L (\rho_i + \pi_i) = 1$ . Nevertheless, the current differs from that of the equivalent one-lane model only by a positive  $O(1)$  factor. This loose formulation of the correspondence will be sufficient for latter reasoning as the only information we need is

the sign of the current. For the equivalent one-lane model a potential  $U_i^A$  at site  $i$  can be defined by  $\Delta U_i \equiv U_i^A - U_{i-1}^A = \ln(\tilde{q}_i/\tilde{p}_{i-1})$ . This reads in terms of the rates of the two-lane model:

$$\Delta U_i \equiv U_i^A - U_{i-1}^A = \ln \frac{q_i(p_i + u_i)}{p_{i-1}(q_i + v_i)}. \quad (5)$$

In fact, the potential itself exists even in the case when not all  $v_i$  are positive. This effective potential can be obtained in a more direct way by considering the steady state of a single particle in a closed system, i.e. open chain with  $\alpha = \beta = \gamma = 0$ . In this case  $J = 0$  and Eqs. (1-3) can be equivalently written as:

$$\rho_{i-1}/\rho_i = \frac{q_i(p_i + u_i)}{p_{i-1}(q_i + v_i)} \quad (6)$$

$$\pi_i/\pi_{i+1} = \frac{q_{i+1}(p_i + u_i)}{p_i(q_i + v_i)} \quad (7)$$

$$\pi_i/\rho_i = \frac{p_i + u_i}{q_i + v_i}. \quad (8)$$

From these relations, one can see that the steady state is identical to that of an equilibrium system, where detailed balance is satisfied and the potential is given by Eq. (5) in lane  $A$  and by  $U_i^B - U_i^A = \ln[(p_i + u_i)/(q_i + v_i)]$  in lane  $B$ . We thus conclude that the motion of a single particle can be effectively described by a one-dimensional motion in the potential  $U_i^A$ .

Next, we examine the dynamics of a single vacancy in the system when all but one of the sites are occupied. It is easy to see that the dynamics of a lonely vacancy differs from that of a lonely particle in that the direction of transitions (i.e. the arrows in Fig. 3) are reversed. This is equivalent with a single particle dynamics analyzed above, however, in a modified environment where the rates  $p_{i-1}$  and  $q_i$  of the original environment are interchanged for all  $i$ . The effective potential  $\bar{U}_i^B$  associated with a single vacancy is thus given by

$$\Delta \bar{U}_i \equiv \bar{U}_i^B - \bar{U}_{i-1}^B = \ln \frac{p_{i-1}(q_{i+1} + u_i)}{q_i(p_{i-1} + v_i)}. \quad (9)$$

In a system which is homogeneous in the bulk a single particle is driven from left to right if  $\Delta U < 0$ , whereas it is driven from right to left if  $\Delta U > 0$ . In the latter case we speak of *reverse bias* and in the followings, we shall focus on this regime. The condition  $\Delta U > 0$  of reverse bias in the bulk reads in terms of jump rates as :

$$q/p > v/u. \quad (10)$$

Note that the potential difference experienced by a vacancy can have any sign in the reverse bias regime. Namely, it is driven to the right if  $\Delta \bar{U} < 0$ , or equivalently if  $q/p > u/v$  while it is driven to the left if  $q/p < u/v$ . This contrasts with the one-lane partially asymmetric exclusion process, where  $\Delta U_i = -\Delta \bar{U}_i$  always holds.

#### 4. Periodic system

Let us consider a homogeneous, periodic system with  $2L$  sites and  $N$  particles. It is straightforward to check that the probability of configurations  $\{n_i^A, n_i^B\}$  is of factorized form in the steady state:

$$P(\{n_i^A, n_i^B\}) = Z^{-1} \left[ \prod_{i=1}^L \rho^{n_i^A} (1-\rho)^{1-n_i^A} \pi^{n_i^B} (1-\pi)^{1-n_i^B} \right] \delta \left( \sum_{i=1}^L (n_i^A + n_i^B), N \right), \quad (11)$$

where  $\delta(i, j)$  is the Kronecker symbol and the factor  $Z \equiv \sum_{\{n_i^A, n_i^B\}} P(\{n_i^A, n_i^B\}) \delta(\sum_{i=1}^L (n_i^A + n_i^B), N)$  ensures normalization. The parameters  $\rho$  and  $\pi$  in Eq. (11) lie in the interval  $(0, 1)$  and satisfy the relation

$$u\rho(1-\pi) = v\pi(1-\rho). \quad (12)$$

Keeping the density of particles  $\varrho \equiv N/(2L)$  constant and performing the thermodynamic limit  $L \rightarrow \infty$ , the factorized form in Eq. (11) results in a simple form of the current:  $J_\infty = p\rho(1-\rho) - q\pi(1-\pi)$ . Here,  $\rho$  and  $\pi$  are fixed by the density through  $\varrho = (\rho + \pi)/2$  and are interpreted as the particle densities in lane  $A$  and  $B$ , respectively. The current, as a function of  $\rho$ , reads as

$$J_\infty(\rho) = \rho(1-\rho) \left[ p - \frac{qv/u}{\rho + (v/u)(1-\rho)^2} \right]. \quad (13)$$

The fundamental diagram of the model, i.e. the current plotted against the density  $\varrho$ , can be seen in Fig. 4. Depending on the bulk rates, one can distinguish between two

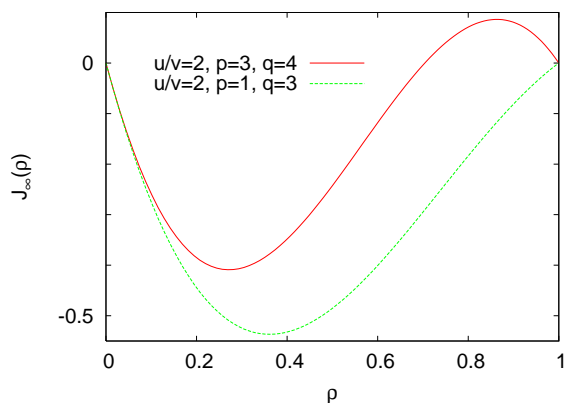


**Figure 4.** The current as a function of the particle density  $\varrho$  for two different set of bulk rates.

domains of the parameter space in the reverse bias regime, which are characterized by qualitatively different shape of the curve  $J(\varrho)$ . It is straightforward to show that if

$$q/p > u/v, \quad (14)$$

the fundamental diagram has a single extremum (minimum) and the current is negative for any density  $0 < \varrho < 1$ . If condition (14) holds, we shall speak of a *strong bias* (SB).

Note that inequalities (10) and (14) imply that  $q > p$  is a necessary condition of strong bias. If, however,

$$q/p < u/v \quad (15)$$

holds, there exists a non-trivial density  $\varrho_0$  in the interval  $(0, 1)$ , at which the current is zero, i.e.  $J_\infty(\varrho_0) = 0$ . The corresponding densities in lane  $A$  and  $B$  can be easily calculated:

$$\rho_0 = \left( \sqrt{\frac{qv}{pu}} - \frac{v}{u} \right) \left( 1 - \frac{v}{u} \right)^{-1}, \quad \pi_0 = \sqrt{\frac{pu}{qv}} \rho_0. \quad (16)$$

In this case, the fundamental diagram has two extrema (a maximum and a minimum) and, for high enough densities ( $\varrho_0 < \varrho < 1$ ), the current is positive. If inequality (15) is satisfied, we shall speak of a *weak bias* (WB). Inequalities (10) and (15) imply that the necessary condition of weak bias is  $v < u$ . Recalling the dynamics of a single vacancy discussed in the previous section, we can see that, in the strong bias regime, the vacancy is driven from left to right ( $\Delta\bar{U} < 0$ ), whereas, in the weak bias regime, it is driven from right to left ( $\Delta\bar{U} > 0$ ). The connection between the direction of motion of a single vacancy and the shape of the fundamental diagram can be immediately seen. If the vacancy moves from left to right ( $\Delta\bar{U} < 0$ ), the current is negative for finite  $L$  and  $N = 2L - 1$ . Therefore the slope of the curve  $J_\infty(\varrho)$  must be negative at  $\varrho = 1$ , i.e.  $\lim_{\varrho \rightarrow 1} \frac{dJ_\infty(\varrho)}{d\varrho} < 0$ . If the vacancy moves from right to left ( $\Delta\bar{U} > 0$ ), the current is positive and  $\lim_{\varrho \rightarrow 1} \frac{dJ_\infty(\varrho)}{d\varrho} > 0$ .

In the borderline case  $q/p = u/v$ , the motion of a vacancy is diffusive ( $\Delta\bar{U} = 0$ ) and  $\lim_{\varrho \rightarrow 1} \frac{dJ_\infty(\varrho)}{d\varrho} = 0$ . Apart from this anomaly at  $\varrho = 1$ , the shape of the fundamental diagram is similar to that in the strong bias regime.

## 5. Open system

In this section, we shall investigate the steady state of an open system in the reverse bias regime, i.e. when the bulk rates satisfy inequality (10).

First, we recall the steady state of the one-lane partially asymmetric simple exclusion process in the reverse bias regime ( $q > p$ ) [34, 33, 13]. For finite injection rate and zero exit rate at site 1, an anti-shock (or domain wall) develops in the density profile, where the density changes rapidly with the position (see Fig. 5). As a consequence of particle-hole symmetry of this model, the anti-shock is located in the middle of the system. With the distance measured from the middle of the system, the density tends exponentially to one(zero) on the left(right) hand side of the anti-shock, and the shock region, where the density differs significantly from the bulk value has a characteristic width  $\xi \sim 1/\Delta U = 1/\ln(q/p)$ . The stationary current decreases with the system size as  $J(L) \sim e^{-L\Delta U/2}$  and tends to zero in the limit  $L \rightarrow \infty$  [13].

Returning to the two lane model, let us investigate the possibility of an anti-shock type steady state. In the low density domain (i.e. on the right hand side of the domain wall) and far away from the shock region, particles meet each other very

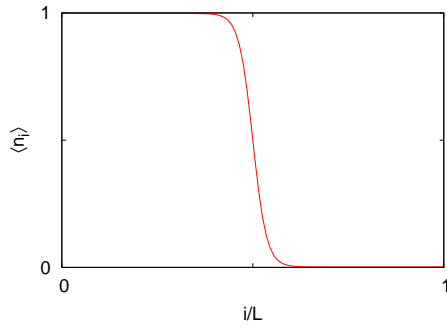


**Figure 5.** Schematic density profile of the one-lane partially asymmetric simple exclusion process in the reverse bias regime  $q > p$ .

rarely. Therefore, they can be regarded as freely moving particles. The same is true for vacancies in the high density domain (i.e. on the left hand side of the anti-shock). Within the frame of this phenomenological description, we can formulate necessary conditions of the stability of the domain wall. First, particles which have come off from the high density domain and penetrated into the low density domain must be driven back to the high density domain. This condition is equivalent to  $\Delta U > 0$  or, in terms of jump rates, to inequality (10), so it is always satisfied in the reverse bias regime. Second, vacancies which penetrate into the high density domain must be driven back to the low density domain. This condition is equivalent to  $\Delta \bar{U} < 0$  or, in terms of jump rates, to inequality (14). We thus conclude that an anti-shock type steady state in the reverse bias regime is possible only in the case of a strong bias. This analysis shows that the steady state of the model for strong bias and for weak bias are much different; therefore the two cases will be discussed separately.

### 5.1. Strong bias

First, we assume that the bias is strong, i.e. the bulk rates satisfy inequality (14). The exit rate  $\gamma$  is set to 1 and we are interested in the steady state for given boundary rates  $\alpha > 0$  and  $\beta$ . Although, we could not find the exact form of the steady state, the shape of the density profile on a macroscopic scale and the leading size dependence of the current can be obtained by means of phenomenological arguments. As the localized domain wall is stable for strong bias we expect the density profile to be qualitatively similar to that of the one-lane partially asymmetric simple exclusion process. For  $\beta = 0$  and for any  $\alpha > 0$ , an anti-shock develops in the interior of the system, which separates a high density domain from a low density domain. The center of the shock region is located at some  $0 < l^* < L$  and the density tends exponentially to zero(one) in the low(high) density domain on a characteristic scale  $\xi \sim 1/\Delta U$  ( $\bar{\xi} \sim 1/|\Delta \bar{U}|$ ). The position of the domain wall  $l^*$  is determined by the condition that, at stationarity, the traveling time of particles from the shock region to site  $L$  must equal to the traveling time of vacancies through the high density domain to site 1, otherwise the domain wall would move with

a finite velocity. Thus, for  $\xi, \bar{\xi} \ll L$ , we may write

$$e^{l^*|\Delta\bar{U}|} \sim e^{(L-l^*)\Delta U}. \quad (17)$$

Introducing the fraction  $r$  of the system which is occupied by the high density domain in the limit  $L \rightarrow \infty$ , i.e.  $r \equiv \lim_{L \rightarrow \infty} l^*(L)/L$ , Eq. (17) yields:

$$r = \left(1 + |\Delta\bar{U}|/\Delta U\right)^{-1} = \left(1 + \ln \frac{q(p+v)}{p(q+u)} / \ln \frac{q(p+u)}{p(q+v)}\right)^{-1}. \quad (18)$$

As can be seen, unlike for the one-lane partially asymmetric simple exclusion process,  $r$  differs from  $1/2$  if  $u \neq v$ , which is the consequence of the breaking of the particle-hole symmetry. For large  $L$ , the stationary current, which is proportional to the inverse of traveling time, tends exponentially to zero with increasing system size:

$$J(L) \sim e^{-\Delta U(1-r)L} = \left(\frac{q(p+v)}{p(q+u)}\right)^{(1-r)L}. \quad (19)$$

If  $\beta > 0$  (and  $\alpha > 0$ ), the high density domain shrinks to the left boundary of the system; in other words, the low density domain extends over the entire system and a boundary layer forms at the left boundary. The width of the boundary layer increases with decreasing  $\beta$  but remains finite for finite  $\beta$ , which means that  $r = 0$ . The expression of the current in Eq. (19) is valid with  $r = 0$ .

## 5.2. Marginal bias

Next, the marginal case is considered, when  $q/p = u/v$  or, equivalently,  $\Delta\bar{U} = 0$ . From Eq. (18) we obtain  $r = 1$ . Therefore, if  $\beta = 0$  and  $\alpha > 0$  the high density domain extends over the whole system and a boundary layer forms at the right boundary. The characteristic scale  $\bar{\xi} = 1/|\Delta\bar{U}|$  diverges, therefore the density must tend slower than exponentially to the bulk value. The motion of a single vacancy is diffusive, so, far from the right boundary, where the density of vacancies is close to zero, they can be approximatively regarded as independent, diffusing particles. When a system of independent, diffusing particles is coupled to boundary reservoirs with different densities, the steady state density profile interpolates linearly between the densities of reservoirs. Therefore we conclude that, for sites far away from the right boundary, the profile is linear:  $1 - \langle n_i^A \rangle \sim i/L$ ,  $1 - \langle n_i^B \rangle \sim i/L$ ,  $i \ll L$ . It follows then that the current is inversely proportional to the system size:

$$J(L) = \alpha(1 - \langle n_1^A \rangle) \sim L^{-1}. \quad (20)$$

For  $\beta > 0$  (and  $\alpha > 0$ ), the high density domain shrinks to the left boundary ( $r = 0$ ). For a given  $\beta$ , the width of the boundary layer is significantly larger than in the case of strong bias since the profile in the high density domain approaches the bulk value much slower. The current decreases exponentially as given in Eq. (19) with  $r = 0$ .

Numerical simulations are in agreement with the above results obtained for strong and marginal bias.

### 5.3. Weak bias

Next, we turn to the case of weak bias in the bulk. According to numerical simulations, the open system has three phases, see the phase diagram in Fig. 6. If the exit rate

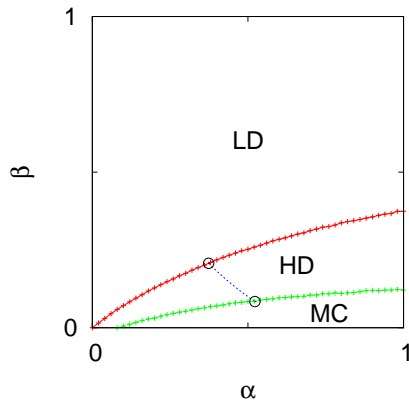


**Figure 6.** Phase diagram of the open system with weak (reverse) bias. The bulk rates are  $p = 2/3$ ,  $q = 1$ ,  $u = 3/4$  and  $v = 1/4$ . The low density, high density and maximum current phase are denoted by LD, HD and MC, respectively. The boundaries of the high density phase have been calculated by numerical simulations. Along the dashed line given in Eq. (23), the semi-infinite system has a product measure steady state. The circles denote the exactly known points of the phase boundaries.

exceeds a certain  $\alpha$ -dependent value,  $\beta_1(\alpha)$ , the effective injection rate of particles at the left boundary is not sufficiently large to force a non-vanishing current against the bias in the bulk. The low density domain covers the entire system ( $r = 0$ ) and a boundary layer forms at the left boundary. The current decreases exponentially with  $L$  as given in Eq. (19) with  $r = 0$ . This phase is termed as low density (LD) phase. If  $\beta$  is smaller than  $\beta_1(\alpha)$  the particle injection at the left boundary is able to force a finite density  $\varrho > \varrho_0$  to the bulk. At both ends of the system, boundary layers form but, far from the boundaries, the profiles tend exponentially to constant values  $\rho$  and  $\pi$  in lane  $A$  and  $B$ , respectively, which fulfill relation (12). Thus, in the bulk of a large system, the influence of boundary layers can be neglected. To be precise, the steady state of a finite open subsystem in the middle of the system,  $[L/2 - a, L/2 + a]$ , is of factorized form in the limit  $L \rightarrow \infty$ :  $P(\{n_i^A, n_i^B\}) = \prod_{i=L/2-a}^{L/2+a} \rho^{n_i^A} (1 - \rho)^{1-n_i^A} \pi^{n_i^B} (1 - \pi)^{1-n_i^B}$ . As a consequence, the current is given by Eq. (13) in the limit  $L \rightarrow \infty$  and, in accordance with  $\varrho > \varrho_0$ , it is non-vanishing:  $J_\infty \equiv \lim_{L \rightarrow \infty} J(L) > 0$ . In this phase, which is termed as high density (HD) phase, the bulk densities  $\rho$  and  $\pi$ , as well as the current are non-trivial functions of  $\alpha$  and  $\beta$ .

At the phase boundary between the LD and the HD phase ( $\beta = \beta_1(\alpha)$ ), a similar phenomenon can be observed as at the coexistence line of the one-lane ASEP. The HD and the LD phase coexist here in the sense that a delocalized anti-shock develops in the interior of the system, which separates a HD domain on its left hand side from a LD domain on its right hand side. At the left end of the system, exponentially decaying

boundary layers develop in the profiles. In the bulk of the HD domain, the densities are  $\rho_0$  and  $\pi_0$  given in Eq. (16), which follows from that  $J_\infty = 0$ . In the bulk of the LD domain, the densities are zero:  $\rho = \pi = 0$ . The anti-shock has a finite width and its center performs symmetric diffusion in the whole system. A symmetric random walk on a one-dimensional lattice of size  $L$  with reflective boundaries has a steady state with a uniform probability  $1/L$  at each site. For a sharp domain wall and no boundary layer at the left end this would lead to profiles which interpolate linearly between  $\rho_0(\pi_0)$  and zero in lane  $A(B)$ . For a finite system this holds only approximatively for large  $L$  and far from the boundaries:  $\langle n_i^A \rangle \approx (1 - i/L)\rho_0$ ,  $\langle n_i^B \rangle \approx (1 - i/L)\pi_0$ ,  $1 \ll i \ll L$ . Nevertheless, on the macroscopic scale, i.e. introducing the rescaled variable  $x = i/L$  and performing the limit  $L \rightarrow \infty$ , the profiles are given as:

$$\langle n_x^A \rangle = (1 - x)\rho_0, \quad \langle n_x^B \rangle = (1 - x)\pi_0 \quad (21)$$

for  $0 < x < 1$ . The dependence of the current on the system size  $L$  can be easily obtained. Measuring the current at the right end of the system, it is clear that particles have a significant chance to leave the system at the right boundary and contribute to the mean current only when the domain wall is found in the vicinity of the right boundary. The probability of this event is proportional to  $L^{-1}$ , therefore the current in a finite system decreases with  $L$  as:

$$J(L) \sim L^{-1}. \quad (22)$$

In the HD phase, the current  $J_\infty$  is determined by the boundary rates at the left boundary and, for a fixed  $\alpha$ , it increases with decreasing  $\beta$ . For given bulk rates, however, the current which can flow in the bulk is bounded and has a maximal value  $J_{\max}$ , see the fundamental diagram in Fig. 4. Therefore, if  $\alpha$  is not too small and  $\beta$  is decreased the current attains its maximum at some  $\beta = \beta_2(\alpha) > 0$ . If  $\beta_2(\alpha) > 0$  and  $\beta < \beta_2(\alpha)$ , the current is saturated, i.e.  $J_\infty = J_{\max}$ , and the bulk densities  $\rho_{\max}$  and  $\pi_{\max}$  in lane  $A$  and  $B$ , respectively, are given by the equation  $J_\infty(\rho_{\max}) = J_{\max}$  and by Eq. (12). These densities, as well as the current are independent of the boundary rates  $\alpha$  and  $\beta$ . The density profiles tend algebraically to the bulk value with the distance  $l$  measured from the boundaries as  $|\langle n_l^A \rangle - \rho| \sim l^{-1/2}$ ,  $|\langle n_l^B \rangle - \pi| \sim l^{-1/2}$  for  $1 \ll l \ll L$ . The value of the decay exponent  $1/2$  is related to that the fundamental diagram is quadratic in the vicinity of the maximum [10]. After the analogous phase of the ASEP, this phase will be called maximum current (MC) phase.

In general, we could not determine the phase boundaries  $\beta_1(\alpha)$  and  $\beta_2(\alpha)$  exactly apart from certain special cases. For a given set of bulk rates, we have performed numerical simulations for different boundary rates  $\alpha$  and  $\beta$  and estimated the phase boundaries by measuring the current in the steady state. The results are shown in Fig. 6. The system size and simulation time was  $L = 300$  and  $t = 2 \times 10^6$ , respectively, in case of the upper boundary  $\beta_1(\alpha)$ , whereas  $L = 1000$  and  $t = 5 \times 10^6$  in case of the lower boundary  $\beta_2(\alpha)$ .

A special case, where the upper boundary can be determined exactly is  $p = q$ . If vacancies(particles) in lane  $B$  are regarded as particles(vacancies), one can see that none

of the two lanes is singled out if  $\alpha = \beta$ . The rates at the left boundary thus force a high density domain to the system in which  $\langle n_i^A \rangle_{HD} = 1 - \langle n_i^B \rangle_{HD}$  holds. Here, the subscript HD refers to that the average is restricted to configurations where site  $i$  lies in the high density domain, i.e.  $i \ll l$  where  $l$  is the location of the domain wall. Thus, in the bulk of the high density domain  $\rho = 1 - \pi$  and the corresponding current is zero. Therefore the phase boundary curve  $\beta_1(\alpha)$  coincides in this special case with the diagonal  $\alpha = \beta$ .

Furthermore, there is a line in the phase diagram, where the semi-infinite system has a product measure steady state. It is easy to see that if the densities of particle reservoirs  $\rho = \alpha/p$  and  $\pi = 1 - \beta/q$  are compatible in the sense that they fulfill Eq. (12), moreover, the system is in the HD phase, i.e.  $\rho_0 < \alpha/p < \rho_{\max}$ , then any finite open subsystem  $[1, a]$  ( $a < \infty$ ) has a factorized steady state in the limit  $L \rightarrow \infty$  with homogeneous densities  $\rho$  and  $\pi$  in lane  $A$  and  $B$ , respectively. Expressing the densities of boundary reservoirs with the boundary rates and substituting them in Eq. (12), we obtain

$$\beta_{\text{fact}}(\alpha) = q \left( 1 + \frac{u}{v} \frac{\alpha}{p - \alpha} \right)^{-1}. \quad (23)$$

This curve is plotted in the phase diagram in Fig. 6. On this line, there is no boundary layer at the left boundary. The upper phase boundary is reached at  $\alpha = p\rho_0$ , i.e.  $\beta_1(p\rho_0) = \beta_{\text{fact}}(p\rho_0)$ , whereas the lower phase boundary is reached at  $\alpha = p\rho_{\max}$ , i.e.  $\beta_2(p\rho_{\max}) = \beta_{\text{fact}}(p\rho_{\max})$ . This provides one exactly known point of each phase boundary curve, which are shown in Fig. 6.

## 6. Inhomogeneous model

In the rest of this work, we shall investigate the steady state of the model in the case where the system is heterogeneous, which means that the jump rates are site-dependent. If the bulk rates are random variables, one can easily imagine that there may be both regions where particles feel a local forward bias and regions with a local reverse bias. Such a situation has been studied in the disordered one-lane partially asymmetric simple exclusion process [40, 35, 36, 37, 38, 39]. Note that, in the totally asymmetric process, such a situation cannot be realized. The key to the understanding of such heterogeneous models at a phenomenological level is the steady state of a one-barrier system, i.e. when a homogeneous region with a reverse bias is embedded in a homogeneous medium with a forward bias.

### 6.1. One-barrier system

Let us consider a periodic system of size  $\mathcal{L}$ , which is composed of a homogeneous subsystem (called barrier) with a reverse bias ( $\Delta U > 0$ ), which contains sites  $i = 1, 2, \dots, L$  and the rest of the system (the environment), where there is a forward bias ( $\Delta U < 0$ ). The particle density  $\varrho = N/(2\mathcal{L})$  is fixed, furthermore, we assume that  $1 \ll L = b\mathcal{L}$ , where  $b \ll 1$ , thus the barrier is only a small part of the system so that a

single particle has a positive average velocity (in a finite system). Similar to the reverse bias regime, one must distinguish between two types of forward bias. If  $\Delta U < 0$  and  $\Delta \bar{U} > 0$ , we speak of strong forward bias, while if  $\Delta U < 0$  but  $\Delta \bar{U} < 0$  we speak of weak forward bias. Depending on whether the bias is strong or weak at the barrier and in the environment we have four different cases.

Let us assume that the bias is strong in both parts of the system. In this case, almost all particles are found in a high density cluster of length  $l \simeq N/2 = \rho \mathcal{L}$ , where  $\rho = \pi = 1$ , see Fig. 7a. The right edge of the HD domain (the anti-shock) lies in the barrier region and covers a fraction  $r$  of this region as given in Eq. (18), provided the number of particles is sufficiently large:  $N/2 \simeq l > 2rL$ . Focusing on the barrier region, the steady state is similar to that of an open system with  $\alpha > 0$  and  $\beta = 0$ . If, however,  $N/2 < 2rL$  the HD cluster is located symmetrically on the two sides of site 1 and covers only a fraction  $r = l/(2L) = N/(4L)$  of the barrier region. The stationary current decreases exponentially with  $L$  as given in Eq. (19).

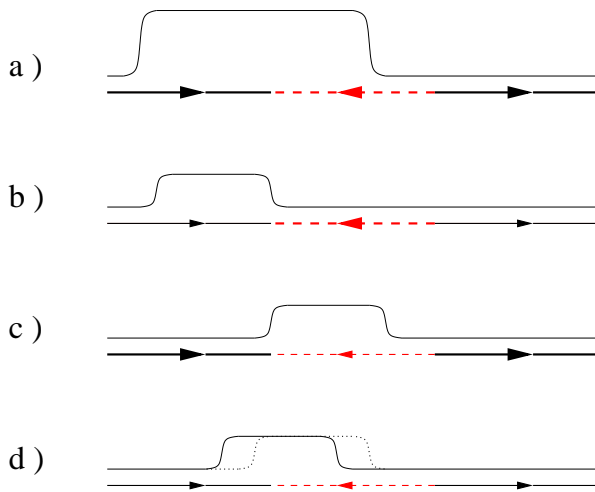


**Figure 7.** Density profiles in different one-barrier systems. Arrows indicate the direction of the bias and big(small) arrow heads correspond to strong(weak) bias.

Next, we consider the case when the bias is still strong in the reverse bias region but it is weak in the environment. Now, a HD cluster forms in the forward bias region, the right edge of which is located at site 1, see Fig. 7b. In the HD domain, the densities  $\rho_0$  and  $\pi_0$  are given by Eq. (12) with the rates of the forward bias region. As particles detaching from the anti-shock region must overcome the empty barrier region, the stationary current is exponentially vanishing, as given in Eq. (19) with  $r = 0$ .

Let us consider the case when the bias is strong in the environment but it is weak in the barrier region. Reversing the directions left and right, this arrangement is identical to the previous one, except that the barrier region is limited. Nevertheless, until  $N < 2L\rho_0$  or, equivalently, if the length  $l = N/(2\rho_0)$  of a HD cluster with density  $\rho_0$  is less than  $L$ , a HD domain will form in the reverse bias region as we have known in the previous case. This is illustrated in Fig. 7c. At the left edge of the HD domain (at site 1), a

boundary layer forms in the forward bias region, which effectively closes the reverse bias region, and the situation is similar to the open system with  $\alpha = \beta = 0$ . Since, the right edge of the HD cluster does not reach the right edge of the barrier region, the current is exponentially vanishing as given in Eq. (19) with  $r = l/L$ . The steady state is, however, different if  $N > 2L\rho_0$ . In this case, the HD domain covers the entire reverse bias region and, here, the density exceeds  $\rho_0$ . Besides, the density of particles is non-vanishing also in the environment and, accordingly, the current is non-vanishing ( $J_\infty > 0$ ), as well.

The most complex situation is when the bias is weak both in the barrier region and in the environment. Restricting our attention to the reverse bias region, this can be regarded as an open system of size  $L$ , with some effective boundary rates  $\alpha_{\text{eff}}$  and  $\beta_{\text{eff}}$ , which depend on the bulk rates in a non-obvious way owing to the presence of boundary layers around site 1. Since both effective boundary rates are finite, the determination of the steady state in the general case is, in addition to the above difficulties, as hard as the determination of the phase diagram for an open system with weak reverse bias. We shall therefore restrict ourselves to the description of the possible steady states and omit to give criteria in terms of the jump rates except of some special cases when the symmetries of the model can be exploited.

For almost all points of the parameter space spanned by  $p_f, q_f, u_f, v_f, p_r, q_r, u_r, v_r$ , where the index  $f(r)$  refers to the forward(reverse) bias region, the steady state is similar to those described in the previous two cases. That means, a high density cluster forms which is located either entirely in the forward bias region (Fig. 7b) or entirely in the barrier region (Fig. 7c) and the densities are given by the densities  $\rho_0$  and  $\pi_0$  of the medium which correspond to zero current, see Eq. (16). In the latter case, the current can be non-vanishing ( $J_\infty > 0$ ) if the density of particles is sufficiently high.

In addition to the above steady states, there is a zero measure set in the parameter space for which the high density cluster becomes delocalized, analogous to the behavior at the phase boundary between the LD and the HD phase in the open system (see Fig. 7d). In this case, the right edge of the high density cluster lies in the reverse bias region and the whole cluster performs symmetric diffusive motion so that the right edge of the cluster moves in the range  $[1, \min\{L, l_r\}]$ , where  $l_r = N/(2\rho_0^r)$  is the length of the cluster corresponding to the zero-current density  $\rho_0^r$  in the reverse bias region. In the part of the cluster which lies in the forward (reverse) bias region, the local densities assume the zero-current densities of the underlying medium, i.e.  $\rho_0^f$  and  $\pi_0^f$  ( $\rho_0^r$  and  $\pi_0^r$ ). If  $l_r/L = \varrho/(b\rho_0^r) \geq 1$ , then the current vanishes with the size of the barrier region as  $J(L) \sim L^{-1}$ , otherwise it decreases exponentially. The symmetric diffusive motion of the cluster results in a linearly decaying average density profile in the barrier region.

The general condition of such a delocalized steady state is not known but we can provide two sufficient conditions, which are related to the symmetries of the model. First, if  $p_f = q_r$ ,  $q_f = p_r$ ,  $u_f = v_r$  and  $v_f = u_r$  then the two sides of site 1 (i.e. the forward bias region and the reverse bias region) are mapped to each other by rotating the system by 180 degrees about the axis perpendicular to the plane in which it is drawn in Fig. 1. That means that the two regions are equivalent and the currents in the two

lanes cancel, independent of the actual location of the HD cluster. Fluctuations of the net current lead to displacements of the latter and, as a consequence, it is delocalized in the steady state. Second, if  $p_f = q_f = p_r = q_r$ , the high density cluster is delocalized again, independent of the lane change rates. This latter case is related to the symmetry already mentioned in Sec. 5.3. When the particles(vacancies) in lane  $A$  are regarded as vacancies(particles) then the particles in both lanes move in the same direction and lane change of the original model transforms to pair annihilation and creation. If the above condition is satisfied the lanes in the transformed model are equivalent. Therefore, the particle currents in the two lanes of the original model compensate each other independent of the location of the particle cluster, which leads to delocalization. Although, boundary layers develop around site 1 in the profiles in lane  $A$  and  $B$ , for the total density  $\langle n_i^A \rangle_{HD} + \langle n_i^B \rangle_{HD} = 1$  holds in the HD cluster due to the above symmetry.

We have performed numerical simulations in the second case and measured the stationary density profiles (see Fig. 8), as well as the current for different system sizes. The results on the current, which are shown in Fig. 9, are in agreement with the law  $J(L) \sim L^{-1}$  for large system sizes. The intercept  $L^*$  of the linear asymptote  $J^{-1}(L) \simeq s(L - L^*)$  with the  $x$  axis can be interpreted as the effective width of the anti-shock region. As can be seen, for smaller  $v_r/u_r$ , the anti-shock is sharper and the finite size corrections to the asymptotic law are weaker. The slope  $s$  of the asymptote depends on  $v_r/u_r$ , as well, through the sharpness of the anti-shock.

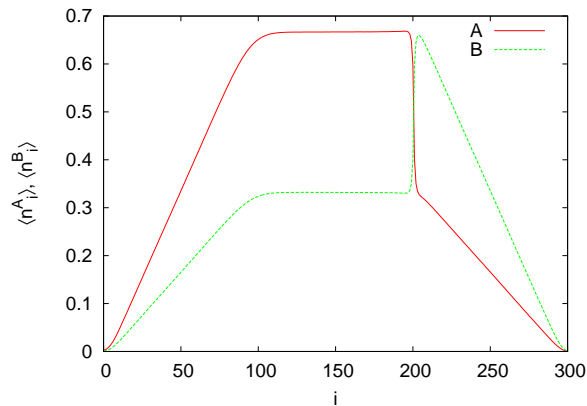


**Figure 8.** Numerically calculated density profiles in a periodic one-barrier system. The size of the system is  $\mathcal{L} = 800$ , the number of particles is  $N = 100$  and the reverse bias region is located in the interval  $[200, 300]$ . Transition rates are  $p_f = q_f = p_r = q_r = 0.5$  and  $v_r = 1 - u_r = u_f = 1 - v_f$ . The simulation time was  $10^9$ . Only the part of the system is shown where the density is significantly differs from zero. In the rest of the system, which is never reached by the high density cluster, the density is vanishing:  $\varrho \approx J/[p_f(v_f - u_f)] \sim \mathcal{L}^{-1}$ .

## 6.2. Disordered system

Next, we shall study the model in the presence of disorder, where the transition rates are site-dependent quenched random variables. The general case is rather complex

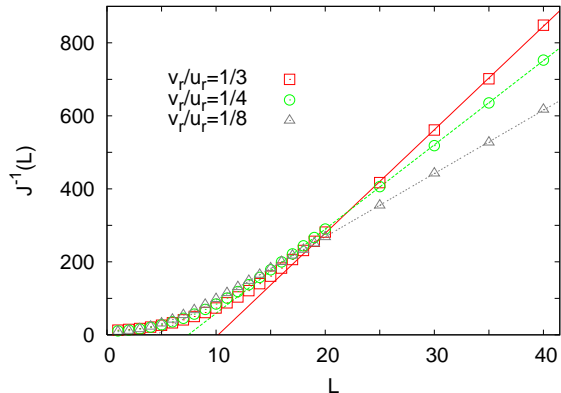


**Figure 9.** The inverse of the measured stationary current as a function of the size  $L$  of the barrier in a periodic one-barrier system for different lane change rates. The size of the system was  $\mathcal{L} = 16L$  and the number of particles was  $N = 4L$ . Transition rates are  $p_f = q_f = p_r = q_r = 0.5$  and  $v_r = 1 - u_r = u_f = 1 - v_f$ . The simulation time was  $10^9$ .

as, in such systems, both weak and strong bias regions may form. We shall therefore restrict the quantitative analysis to two special cases where either exclusively strong or exclusively weak bias regions are found in the system.

*6.2.1. Longitudinal disorder* First, let us consider the case where the lane change rates are homogeneous, i.e.  $u_i = v_i \equiv u$  ( $i = 1, 2, \dots, L$ ) while the other rates  $p_i$  and  $q_i$  are independent quenched random variables. The model with such a *longitudinal disorder* may describe traffic of molecular motors on heterogeneous tracks containing defects where the advance of motors is hindered.

In this case, the potential difference  $\Delta U_{ij}$  between site  $i$  and  $j (> i)$  felt by a particle and the corresponding potential difference  $\Delta \bar{U}_{ij}$  of a vacancy are related as:

$$\Delta U_{ij} = -\Delta \bar{U}_{ij} + \ln \frac{(p_j + u)(q_{j+1} + u)}{(p_i + u)(q_{i+1} + u)}. \quad (24)$$

The second term on the r.h.s. is an  $O(1)$  random variable (with zero mean), which is negligible for large  $j - i$  compared to the first term which increases linearly with  $j - i$  in the case of a global bias and increases as  $\sim \sqrt{j - i}$  in the absence of a global bias. Thus the two potentials are asymptotically perfectly correlated:

$$\Delta U_{ij} \simeq -\Delta \bar{U}_{ij}. \quad (25)$$

As a consequence, there are only strong (forward or reverse) bias regions but no weak bias regions in the case of longitudinal disorder. This is the case also in the disordered one-lane partially asymmetric simple exclusion process, therefore the model behaves similar to that one and we can make use of the known results on that model.

In the following, we assume that the potential landscape is tilted, i.e.  $[\Delta U_i]_{\text{av}} < 0$ , where  $[\cdot]_{\text{av}}$  denotes average over the distribution of jump rates. A given realization of the random potential  $U_i$ ,  $i = 1, 2, \dots, L$  can be regarded as a random walk of  $L$  steps

with step lengths  $\Delta U_i$ , in the presence of a bias in the negative direction. The effective reverse bias regions in the potential landscape can be identified with the ascending parts of Brownian excursions in the positive direction [37, 39]. A Brownian excursion of length  $n$  is a random walk  $U_i$ ,  $i = 0, 1, \dots, n$ , which satisfies that  $U_n = U_0$  and  $U_i > U_0$  for  $0 < i < n$ . The amplitude of the excursion is defined as  $U_{\max} - U_0 \equiv \max_{0 \leq i \leq n} U_i - U_0$ . The effective reverse bias region is identified with the part of the excursion from  $i = 0$  up to the first maximum:

$$l \equiv \min_{0 \leq j \leq n} \{j | U_j = U_{\max}\}. \quad (26)$$

In the steady state of a finite system, the current is determined by the reverse bias region with the largest amplitude  $\Delta U_{\text{MAX}}$ , behind which the particles accumulate and form a high density cluster, where the density is close to 1. Due to the particle-hole symmetry, which is reflected by Eq. (25), half-filling is realized in this maximal reverse bias region, i.e. the anti-shock is located where the potential (measured from the bottom of the barrier) is  $\Delta U_{\text{MAX}}/2$ . The current is therefore given by  $J = 1/\sqrt{\tau_{\text{MAX}}}$ , where  $\tau_{\text{MAX}} = e^{\Delta U_{\text{MAX}}}$  is the waiting time of a single particle in the maximal reverse bias region. The distribution of the amplitudes of Brownian excursions decays asymptotically exponentially (see the Appendix) or, equivalently, the probability density of one-particle waiting times at reverse bias regions has an algebraic tail  $p(\tau) \simeq A\tau^{-1-\mu}$ . Here, the diffusion exponent  $\mu$  is the positive root of the equation  $[(\tilde{q}/\tilde{p})^\mu]_{\text{av}} = 1$  in case of a one-lane system with independent, random rates  $\tilde{p}_i$  and  $\tilde{q}_i$  (see e.g. Ref. [41]). In terms of the jump rates of the original two-lane model, this can be written as:

$$\left[ \left( \frac{q(p+u)}{p(q+v)} \right)^\mu \right]_{\text{av}} = 1. \quad (27)$$

According to extreme value statistical considerations [42], the current, which is related to the largest one-particle waiting time, follows the Fréchet distribution

$$p(\tilde{J}) = 2\mu \tilde{J}^{2\mu-1} e^{-\tilde{J}^{2\mu}}, \quad (28)$$

in terms of the scaling variable  $\tilde{J} = cJ(L)L^{\frac{1}{2\mu}}$ , where the constant  $c$  is related to the prefactor  $A$  of the parent distribution  $p(\tau)$ . The typical current vanishes with the system size  $L$  as:

$$J(L) \sim L^{-1/(2\mu)}. \quad (29)$$

We have performed numerical simulations for the model with rates  $u = 0.5$ ,  $p_i = 1 - q_i$  for all  $i$  and rate  $p_i$  was drawn from a bimodal distribution

$$\rho(p) = c\delta(p - \lambda(1 + \lambda)^{-1}) + (1 - c)\delta(p - (1 + \lambda)^{-1}), \quad (30)$$

with  $\lambda = 0.25$  and  $c = 0.2$ . For this bimodal randomness, the exponent  $\mu$  is given by

$$\mu = \left[ \ln(c^{-1} - 1) \right] \left[ \ln \frac{\lambda + (1 + \lambda)u}{\lambda + \lambda(1 + \lambda)u} \right]^{-1}, \quad (31)$$

which yields  $1/(2\mu) = 0.2767288\dots$  for  $\lambda = 0.25$  and  $c = 0.2$ . We have measured the stationary current in  $10^6$  Monte Carlo steps in  $10^4$  independent samples for system sizes  $L = 2^i$ ,  $i = 8, 9, 10, 11, 12$ . The results on the distribution of the current shown in Fig. 10 are in agreement with the above predictions.

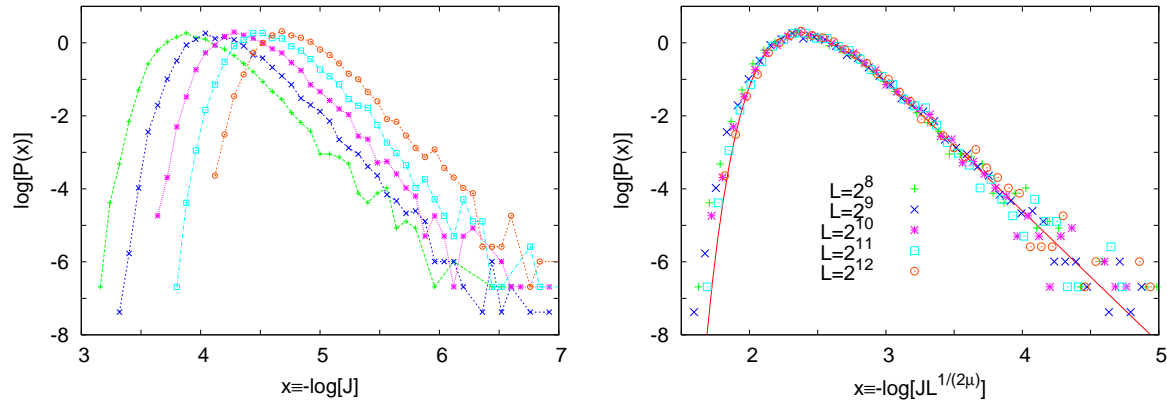


**Figure 10.** Left: Distribution of the logarithm of the current obtained by numerical simulations for different system sizes in case of the bimodal longitudinal disorder given in Eq. (30) with  $\lambda = 0.25$  and  $c = 0.2$ . Right: Scaling plot with the exponent  $1/(2\mu) = 0.2767288 \dots$  predicted by the theory. The solid line is the Fréchet distribution given in Eq. (28).

*6.2.2. Transversal disorder* Let us now consider another type of randomness, where the longitudinal rates are homogeneous, i.e.  $p_i = q_i \equiv p$  for all  $i$ , whereas the transversal rates  $u_i$  and  $v_i$  are random variables. This model will be termed *transversal disorder* and may describe situations where the lane change of molecular motors is biased randomly in space due to the presence of forces transversal to the filament.

In this model, the one-particle potential and one-vacancy potential are again perfectly correlated:

$$\Delta U_i = \Delta \bar{U}_i. \quad (32)$$

Consequently, there are exclusively weak (forward or reverse) bias regions in the system, while strong bias regions are lacking. Let us assume in the following that the potential landscape is tilted, i.e.  $[\Delta U_i]_{\text{av}} < 0$ . Similar to the longitudinal disorder, the environment in which the particles move can be regarded as a set of isolated reverse bias regions which are embedded in a medium with forward bias. We shall apply a phenomenological independent-barrier model to this system, some elements of which have already been mentioned in the previous section. This theory which gives exact results for a single particle in a random environment and results which are in agreement with numerical results for the disordered partially asymmetric simple exclusion process [37], as well as for the present model with longitudinal disorder. The system will be represented by a set of  $L' = O(L)$  consecutive barriers, which exchange particles with each others. There are  $N_i$  particles at the  $i$ th barrier and the barriers are characterized by own current functions  $I_i(N_i)$  which give the current in the one-barrier system with  $N_i$  particles, where the other barriers are deleted. The current  $I_i(N_i)$  is monotonically increasing with  $N_i$  up to a saturation value  $I_i^{\text{max}}$ , i.e.  $I_i(N_i) = I_i^{\text{max}}$  if  $N_i$  is greater than some  $N_i^{\text{max}}$  which is characteristic of the barrier. In what follows, we assume that the total number of particles  $N$  is sufficiently large meaning that  $\sum_i N_i^{\text{max}} < N$ . Then, in the

steady state, the current is determined the barrier with the minimal carrying capacity in the system (indexed by  $m$ ):  $J(L') = \min_i \{I_i^{\max}\} \equiv I_m^{\max}$ . The mean number of particles  $N_i$  at other barriers is determined by  $I_i(N_i) = J(L')$  and  $N_i \leq N_i^{\max}$  for  $i \neq m$ , whereas the number of particles at the saturated barrier is  $N_m = N - \sum_{i \neq m} N_i > N_m^{\max}$ . These particles form a high density cluster behind the saturated barrier, see the density profiles in Fig. 11. As we have seen in the previous section, the transversal disorder

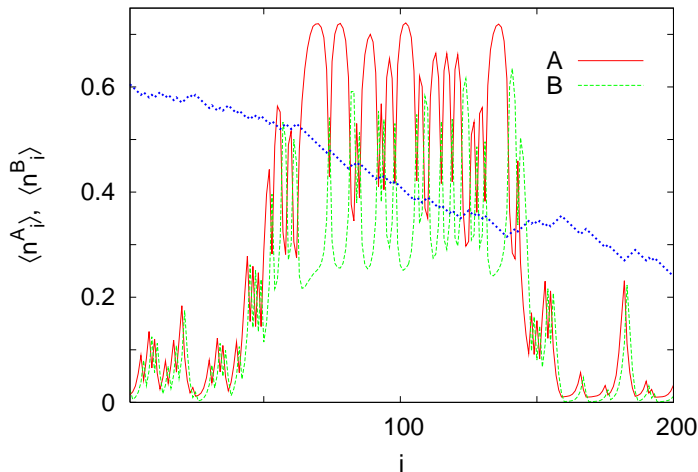


**Figure 11.** Numerically calculated density profiles in the steady state in the presence of transversal disorder. The system size is  $L = 200$  and the number of particles is  $N = 100$ . Bimodal randomness has been used given in Eq. (33) with  $c = 1/3$ ,  $\lambda = 1/8$  and  $p = 0.5$ . The dotted line indicates the potential landscape  $U_i$ . The longest reverse bias region is in the domain  $[139, 170]$ . Behind this region, a high density cluster of approximate length 100 can be observed, where  $\langle n_i^A \rangle + \langle n_i^B \rangle \approx 1$ .

corresponds to the special case, where the high density cluster is delocalized at a barrier. For homogeneous barrier regions, which is a good approximation for bimodal randomness of the type  $u_i = 1 - v_i$ ,

$$\rho(u) = c\delta(u - \lambda(1 + \lambda)^{-1}) + (1 - c)\delta(u - (1 + \lambda)^{-1}) \quad (33)$$

in the limit  $c \ll 1$ , the saturation value of the current (when  $N_i > N_i^{\max}$ ) depends asymptotically on the extension of the barrier region  $l$  as  $[I^{\max}(l)]^{-1} \simeq s(l - l^*)$  where  $s$  and  $l^*$  are common constants for the barriers. Apart from this limit, the barriers are inhomogeneous, i.e. they may contain smaller domains with forward bias, and as a first guess, they are identified with the ascending parts of Brownian excursions of the potential  $U_i$ , just as for longitudinal disorder. Nevertheless, for inhomogeneous barriers, the HD cluster is still delocalized, therefore the saturation value of the current scales with the extension  $l_i$  of the barrier defined in Eq. (26) as  $I^{\max}(l_i) \simeq l_i^{-1}$ . Thus, the current in a finite system is expected to scale as

$$J \sim l_{\max}^{-1}, \quad (34)$$

where  $l_{\max} \equiv \max_{1 \leq i \leq L'} \{l_i\}$  is the length of the longest reverse bias region present in the system.

We have performed numerical simulations for the model with transversal disorder and measured the current in the steady state. We have determined in each sample the size  $l_{\max}$  of the longest effective reverse bias region. Then the measurement was carried out for  $10^5$  independent samples and the average of the logarithm of the current has been calculated over samples where  $l_{\max}$  was the same. The dependence of the calculated typical current  $[J(l_{\max})]_{\text{typ}} = \exp([\ln J(l_{\max})]_{\text{av}})$  on  $l_{\max}$  is shown in Fig. 12. As can be

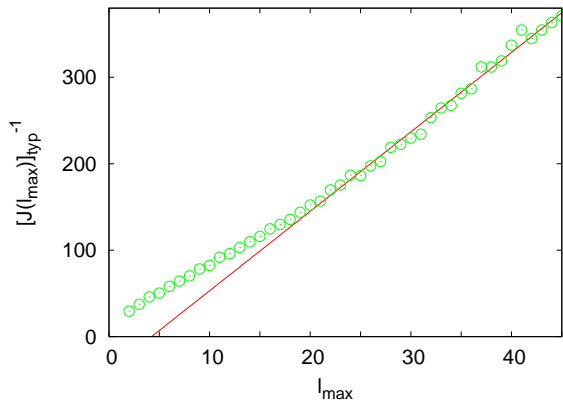


**Figure 12.** Dependence of the typical current on the length of the longest reverse bias region in the model with transversal disorder. The size of the system was  $L = 256$  and bimodal randomness in Eq. (33) has been used with  $c = 1/3$  and  $\lambda = 1/8$ . The number of particles was  $N = 128$ .

seen, the numerical results are in agreement with the law given in Eq. (34). Independent of the precise definition of effective reverse bias regions, one may generally conclude that their probability of occurrence must be exponentially small in their size  $l$  (apart from possible corrections like in the case of continuous-time Brownian excursions [44]) since the majority of the lane change rates in such a region is of that type which results in reverse bias (in the particular case in Eq. (33) that with probability  $c$ ). Therefore, the length of the longest effective reverse bias region scales with the size of the system  $L$  as  $l_{\max} \sim \ln L$ . Finally, we obtain that the current scales with  $L$  in the case of transversal disorder as

$$J(L) \sim (\ln L)^{-1}. \quad (35)$$

We have computed the probability of amplitude  $\Delta U$  of Brownian excursions and the probability of the extension  $l$  of the effective reverse bias region which is given by the time at which the maximum is first assumed in Brownian excursions; for the details of the calculation, see the Appendix. The results are plotted in Fig. 13. The probability of amplitudes, which is the relevant variable in case of longitudinal disorder, tends rapidly to the asymptotical exponential form. Contrary to this, the probability of the extension  $l$  of effective reverse bias regions, which is the important variable in case of transversal disorder, has strong corrections to the exponential for moderate  $l$ . Therefore the asymptotic decay in Eq. (35) is expected to be observed for rather large system sizes which are beyond the realm of numerical simulations.

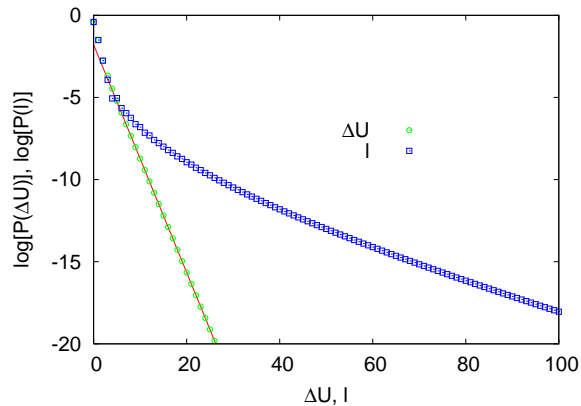


**Figure 13.** Probability of the amplitude  $\Delta U$  (in units  $\ln \frac{p+\lambda/(1+\lambda)}{p+1/(1+\lambda)}$ ) and the probability of the time at which the maximum is first assumed in Brownian excursions corresponding to bimodal randomness with  $c = 1/3$ . Latter quantity is identified with the length  $l$  of effective reverse bias regions. The straight line is the asymptotic form given in Eq. A.3.

## 7. Summary

We have studied in this work a two-lane model that describes bidirectional transport of particles interacting by hard core exclusion. Although, the one-particle dynamics in such a two-channel environment are qualitatively similar to those in a one-lane partially asymmetric system which allows backward steps of the particle, the many particle steady-state behavior can be much different in the two models. We have investigated situations when the track contains regions where the preferred direction of motion of particles is opposite to the global bias. In this case, we have found two types of steady states and have given the conditions of them in terms of the transition rates. In the case of strong reverse bias, which can be induced by making the rates of transitions parallel to the track asymmetric, the steady state is similar to that of the one-lane partially asymmetric exclusion process: a compact, localized cluster of particles forms and the current vanishes exponentially with the extension of the reverse bias region. In case of weak bias, realized by rendering the lane change rates asymmetric, which has no counterpart in the one-lane asymmetric model, a qualitatively different steady state is observed. The cluster of particles becomes now delocalized and, as a consequence, the current vanishes inversely proportionally with the size of the barrier region. We have thus found that, compared to analogous one-lane systems, there may be physically different steady states, in which the flow against the local external drive is facilitated by the cooperative behavior of particles. It is an interesting question whether this type of delocalization can be observed in experiments or in living cells.

## Appendix A.

Let us consider the bimodal randomness given in Eq. (30) and introduce  $x_i \equiv U_i / \ln \frac{p+\lambda/(1+\lambda)}{p+1/(1+\lambda)}$ . This rescaled potential landscape  $\{x_i\}$  is a random walk with steps of unit length with probabilities  $c$  and  $1 - c$  in the positive and negative directions, respectively. Let us assume that the walk starts at  $x_0 = 1$  and absorbing walls are located at  $x = 0$  and at  $x = X + 1 > 1$ . A central quantity in the computation of the statistics of the maximum is the probability that the walker is found after  $t$  steps at site  $x$ :  $P_X(x, t; c)$ . The probability that the walk ends at the absorbing site  $X + 1$  without ever having crossed the starting point is called persistence probability and it is given as  $p_{\text{pers}}(X; c) = \lim_{t \rightarrow \infty} P_X(X + 1, t; c)$ . This quantity can be exactly calculated [43] and reads in the present case:

$$p_{\text{pers}}(X; c) = (1/c - 2)[(1/c - 1)^{X+1} - 1]^{-1}. \quad (\text{A.1})$$

The probability that the amplitude  $x_{\text{max}}$  of the walk before it crosses the wall at  $x = 0$  can be written in terms of the persistence probability as

$$\text{Prob}(x_{\text{max}} = x) = c[p_{\text{pers}}(x - 1; c) - p_{\text{pers}}(x; c)] \quad (\text{A.2})$$

for  $x > 1$ . For  $x = 0$  and  $x = 1$ , we have  $\text{Prob}(x_{\text{max}} = 0) = 1 - c$  and  $\text{Prob}(x_{\text{max}} = 1) = c(1 - c)$ . For large  $x$ , this probability decays exponentially:

$$\text{Prob}(x_{\text{max}} = x) \simeq (1 - 2c)^2 / (1 - c)(1/c - 1)^{-x}. \quad (\text{A.3})$$

Next, we turn to the computation of the distribution of the time  $t_{\text{max}}$  at which the walk first reaches its maximum before it crosses the wall at  $x = 0$ . It is easy to see that  $\text{Prob}(t_{\text{max}} = 0) = 1 - c$  and  $\text{Prob}(t_{\text{max}} = 1) = c(1 - c)$ . For  $t_{\text{max}} > 1$ , the joint probability that the amplitude is  $x_{\text{max}}$  and it is assumed for the first time at time  $t_{\text{max}}$  is given as  $c^2 P_{x_{\text{max}}-1}(x_{\text{max}} - 1, t_{\text{max}} - 2; c) p_{\text{pers}}(x_{\text{max}}; 1 - c)$ . From this, the marginal distribution of  $t_{\text{max}}$  is obtained as

$$\text{Prob}(t_{\text{max}} = t) = c^2 \sum_{x_{\text{max}}=2}^t P_{x_{\text{max}}-1}(x_{\text{max}} - 1, t - 2; c) p_{\text{pers}}(x_{\text{max}}; 1 - c). \quad (\text{A.4})$$

The quantities  $P_X(x, t; c)$  which appear in the above expression can be computed iteratively from those at time  $t - 1$  using the initial condition  $P_X(1, 0; c) = 1$  and  $P_X(x, 0; c) = 0$  for  $x \neq 1$ .

## Acknowledgments

This work has been supported by the Hungarian National Research Fund under grant no. OTKA K75324.

## References

- [1] J. Howard, *Mechanics of Motor Proteins and the Cytoskeleton* (Sinauer, Sunderland, 2001).

- [2] Schliwa M and Woehlke G, 2003 *Nature* **422** 759
- [3] Gross S P, 2004 *Phys. Biol.* **1** R1
- [4] Chowdhury D, Schadschneider A, and Nishinari K, 2005 *Physics of Life Reviews (Elsevier, New York)* Vol. 2, p. 318
- [5] MacDonald C T, Gibbs J H and Pipkin A C, 1968 *Biopolymers* **6** 1
- [6] Spitzer F, 1970 *Adv. Math.* **5** 246
- [7] Liggett T M, 1999 *Stochastic interacting systems: contact, voter, and exclusion processes*, (Berlin, Springer)
- [8] Schmittmann B and Zia R, 1995 in *Phase Transitions and Critical Phenomena*, vol. 17, edited by Domb C and Lebowitz J L (Academic, London)
- [9] Schütz G M, 2001 in *Phase Transitions and Critical Phenomena*, vol. 19, edited by C. Domb and J.L. Lebowitz (Academic, San Diego)
- [10] Krug J, 1991 *Phys. Rev. Lett.* **67** 1882
- [11] Derrida B, Evans M R, Hakim V and Pasquier V, 1993 *J. Phys. A* **26** 1493
- [12] Schütz G M and Domany E, 1993 *J. Stat. Phys.* **72** 277
- [13] Blythe R A, Evans M R, Colaiori F, Essler F H L, 2000 *J. Phys. A: Math. Gen.* **33** 2313
- [14] Pronina E and Kolomeisky A B, 2004 *J. Phys. A: Math. Gen.* **37** 9907; 2006 *Physica A* **372** 12
- [15] Mitsudo T and Hayakawa H, 2005 *J. Phys. A: Math. Gen.* **38** 3087
- [16] Harris R J and Stinchcombe R B, 2005 *Physica A* **354** 582
- [17] Reichenbach T, Franosch T and Frey E, 2006 *Phys. Rev. Lett.* **97** 050603; 2008, *Eur. Phys. J. E* **27** 47; Reichenbach T, Frey E and Franosch T, 2007 *New. J. Phys.* **9** 159
- [18] Jiang R, Hu M B, Wu Y H, Wu Q S 2008, *Phys. Rev. E* **77** 041128
- [19] Cai Z P, Yuan Y M, Jiang R, Hu M B, Wu Q S, Wu Y H 2008, *J. Stat. Mech.* P07016
- [20] Chowdhury D, Santen L, and Schadschneider A, 2000 *Phys. Rep.* **329** 199
- [21] Tsekouras K, Kolomeisky A B 2008, *J. Phys. A: Math Theor.* **41** 465001
- [22] Ebbinghaus M, Santen L 2009, *J. Stat. Mech.* P03030
- [23] Parmeggiani A, Franosch T and Frey E, 2003 *Phys. Rev. Lett.* **90** 086601; 2004 *Phys. Rev. E* **70** 046101
- [24] Lipowsky R, Klumpp S and Nieuwenhuizen T M, 2001 *Phys. Rev. Lett.* **87** 108101
- [25] Klumpp S and Lipowsky R, 2003 *J. Stat. Phys.* **113** 233
- [26] Müller M J I, Klumpp S and Lipowsky R, 2005 *J. Phys.: Condens. Matter* **17** 3839
- [27] Tailleur J, Evans M R and Kafri Y, 2009 *Phys. Rev. Lett.* **102** 118109
- [28] Juhász R, 2007 *Phys. Rev. E* **76** 021117
- [29] Klumpp S and Lipowsky R, 2005 *Phys. Rev. Lett.* **95** 268102
- [30] Konzack S, Rischitor P E, Enke C and Fischer R, 2005 *Mol. Biol. Cell* **16** 497
- [31] Nishinari K, Okada Y, Schadschneider A and Chowdhury D, 2005 *Phys. Rev. Lett.* **95** 118101
- [32] Greulich P, Garai A, Nishinari K, Schadschneider A and Chowdhury D, 2007 *Phys. Rev. E* **75** 041905
- [33] Ramaswamy R and Barma M, 1987 *J. Phys. A: Math. Gen.* **20** 2973
- [34] Sadow S and Schütz G, 1994 *Eurphys. Lett.* **26** 7
- [35] Tripathy G and Barma M, 1997 *Phys. Rev. Lett.* **78** 3039; 1998 *Phys. Rev. E* **58** 1911
- [36] Krug J, 2000 *Braz. J. Phys.* **30** 97
- [37] Juhász R, Santen L and Iglói F, 2005 *Phys. Rev. Lett.* **94** 010601; 2006 *Phys. Rev. E* **74** 061101
- [38] Barma M, 2006 *Physica A* **372** 22
- [39] Juhász R, 2007 *J. Stat. Mech.* P11015
- [40] Koscielny-Bunde E, Bunde A, Havlin S, and Stanley H E, 1988 *Phys. Rev. A* **37** 1821
- [41] Bouchaud J-P and Georges A 1990 *Phys. Rep.* **195** 127
- [42] J. Galambos, 1978 *The Asymptotic Theory of Extreme Order Statistics* (John Wiley and Sons, New York).
- [43] Iglói F and Rieger H 1998 *Phys. Rev. E* **58** 4238
- [44] Randon-Furling J and Majumdar S N 2007 *J. Stat. Mech.* P10008